Electronic Supplementary Information

Efficient photodecomposition of 2,4-dichlorophenol on recyclable phase-mixed hierarchically structured Bi_2O_3 coupled with phosphate-bridged nano-SnO_2

Ning Sun, Yang Qu*, Shuangying Chen, Rui Yan, Muhammad Humayun, Yanduo Liu, Linlu Bai, Liqiang Jing* and Honggang Fu

EXPERIMENTAL

Synthesis of materials

Synthesis of mechanically mixed phase-mixed Bi_2O_3 nanocomposites: According to the mass ratio of α-Bi_2O_3 and β-Bi_2O_3 in BO440 sample (58% of β-Bi_2O_3, 42% of α-Bi_2O_3), 0.042 g bare α-Bi_2O_3 (BO500) and 0.058 g bare β-Bi_2O_3 (BO400) were grinded to form mechanically mixed phase-mixed samples.

Characterization

The XRD patterns of the samples were characterized with Bruker D8 Advance X-ray diffractometer equipped with a graphite monochromatized Cu Kα radiation (γ = 1.541874 Å). The UV-Vis diffuse reflection spectrum (DRS) of the samples were recorded with a Model Shimadzu UV2550 spectrophotometer. Electron microscopy images of the samples were recorded on a JEOL JEM-2100 TEM operated at 200 kV. Scanning electron microscopy (SEM) images were taken using a Hitachi S-4800 instrument (Tokyo, Japan), operated at acceleration voltage of 15 kV. The specific surface area was determined according to the Brunauer-Emmett-Teller (BET) method using a Tristar II 3020 surface area and porosity analyzer (micromeritics). The Fourier-transform infrared (FT-IR) spectra of the samples were collected with a Bruker Equinox 55 Spectrometer, using KBr as diluents. X-ray Photoelectron Spectroscopy (XPS) analysis were carried out using a Kratos-AXIS ULTRA DLD apparatus with Al (Mono) X-ray source, and the binding energies were calibrated with

respect to the signal for adventitious carbon (binding energy = 284.6 eV). The surface photovoltage spectra (SPS) were measured with a home-built apparatus, equipped with a lock-in amplifier (SR830, USA) synchronized with a light chopper (SR540, USA). SPS signal was collected by a lock-in amplier (SR830) synchronized with a light chopper (SR540). The mono-chromatic light was obtained by passing light from a 500W xenon lamp (CHF XQ500W) through a double prism monochromator (SBP300).

Analysis of produced hydroxyl radical amount

0.02 g catalyst was dispersed in 50 mL coumarin aqueous solution (0.001 M). Prior to irradiation, the mixed solution was vigorously stirred for 10 min to achieve an adsorption-desorption equilibrium. After 1 h irradiation by 150 W GYZ220 high-pressure Xenon lamp, the solution was centrifuged and then a certain volume of supernate was transferred into a Pyrex glass cell for the fluorescence measurement of 7-hydroxycoumarin at 332 nm excitation wavelength with an emission wavelength of 456 nm through a spectrofluorometer (Perkin-Elmer LS55).

Evaluation for O_2 temperature-programmed desorption.

O_2 temperature-programmed desorption (TPD) were carry out with the help of a Chemisorption Analyzer, tp 5080 Chemisorb with a thermal conductivity detector (TCD). 50 mg of the catalysts were heated up to 300 °C for 1 h to remove the adsorbed water and then cooled to room temperature, the treatment was carried out under a high purity He as carrier gas with a 30 mL min^{-1} flow rate. The high purity O_2 was inlet with at a flow rate of 30 ml min^{-1} for 60 minutes and maintained at 30 °C. The excess physically adsorbed O_2 on the surface of catalysts was drain away by He as carrier gas and last for 60 minutes at 30 °C. After that, the temperature was increased to 700 °C with a 10 °C min^{-1} heating rate. The desorbed O_2 was analyzed by Chemisorption Analyzer, tp 5080 Chemisorb.

Electrochemical impedance spectra and photocurrent action spectra

Electrochemical impedance spectra (EIS) were conducted in a three-electrode equipped with a Electrochemical Workstation (CHI 660, Shanghai CH Instruments

CO., China) and a frequency range from 0.05 to 10^5 Hz with amplitude of 10 mV (RMS) at the bias of 0.1 V *vs*. Ag/AgCl in 0.5 M L^{-1} Na_2SO_4 electrolyte, using a 300 W Xenon lamp as the light source with a 420 nm cutoff filter. Photocurrent action spectra as function of different excitation wavelength ($\lambda \leq 550$ nm) were performed with monochromatic light from a 500 W xenon lamp passing the monochromator (CM110, spectral products).

Photocatalyticactivities for degrading pollutants

The activities of the samples were evaluated by photodegradation of 2,4-DCP using a 150 W xenon lamp (GYZ220). For 2,4-DCP degradation, 0.1 g power and 2,4-DCP solution (50 mL, 30 $mg \cdot L^{-1}$) were mixed in a 100 ml baker under stirring. Before the photoreactions, the mixed solution was stirred in dark for 0.5 h to reach the balance of adsorption-desorption. The above solution was centrifuged after photoreactions for 1 h and the dark absorption was tested with Shimadzu UV-2550 spectrophotometer at the characteristic optical absorption of 285 nm. Similar procedure was applied for photocatalytic degradation of Rhodamine B, except the characteristic optical absorption at 553 nm.

Measurements of produced intermediates and Cl^- amount.

The various intermediates in the process of 2,4-DCP photo-degradation were obtained by using a typical experiment: 0.1 g catalyst was dispersed in 50 mL of 30 $mg \cdot L^{-1}$ 2,4-DCP solution under lucifugal stirring for 0.5 h. Then, the above mixed solution was irradiated under visible light with a xenon lamp (GYZ220) for 80 min. After regular interval for 20 minutes, a certain volume liquid was taken out for measurement. The concentration of 2,4-DCP was detected with Agilent LC-MS/MS (liquid chromatography tandem mass spectrometry) (6410MS, USA) technique. The fragments of the main reaction intermediate were analyzed through scan mode. The produced Cl^- amount was detected by using a Thermor Dionex ICS-600 IC equipped with an isocratic pump and a dialysis system. A mixture of Na_2CO_3 (4.5 $mmol \cdot L^{-1}$) and $NaHCO_3$ (8.0 $mmol \cdot L^{-1}$) aqueous solutions was taken as the mobile phase. The eluent flow rate was fixed at 0.8 $mL \cdot min^{-1}$. The samples were injected by using a 100

μL PEEK loop. Duplicate runs were performed on chromotography columns (Ion Pac AS23 4.0×250 mm). An AERS 500 eluent suppressor was used in an auto-recycle mode before the detector. Data was acquired and analyzed by Chromeleon V6.8 chromatography data software. The standard stock solution of chloride anions (1000 $\mu g \cdot mL^{-1}$) was purchased by Central Iron And Steel Research Institute. Standard solutions of chloride anions (i.e. 0.05, 0.10, 0.25, 0.50, 0.75 and 1.0 $mg \cdot L^{-1}$) were prepared, and the obtained linear equation: y=2.760c, with the correlation coefficient of 0.9991.

Figures-Supporting information (S)

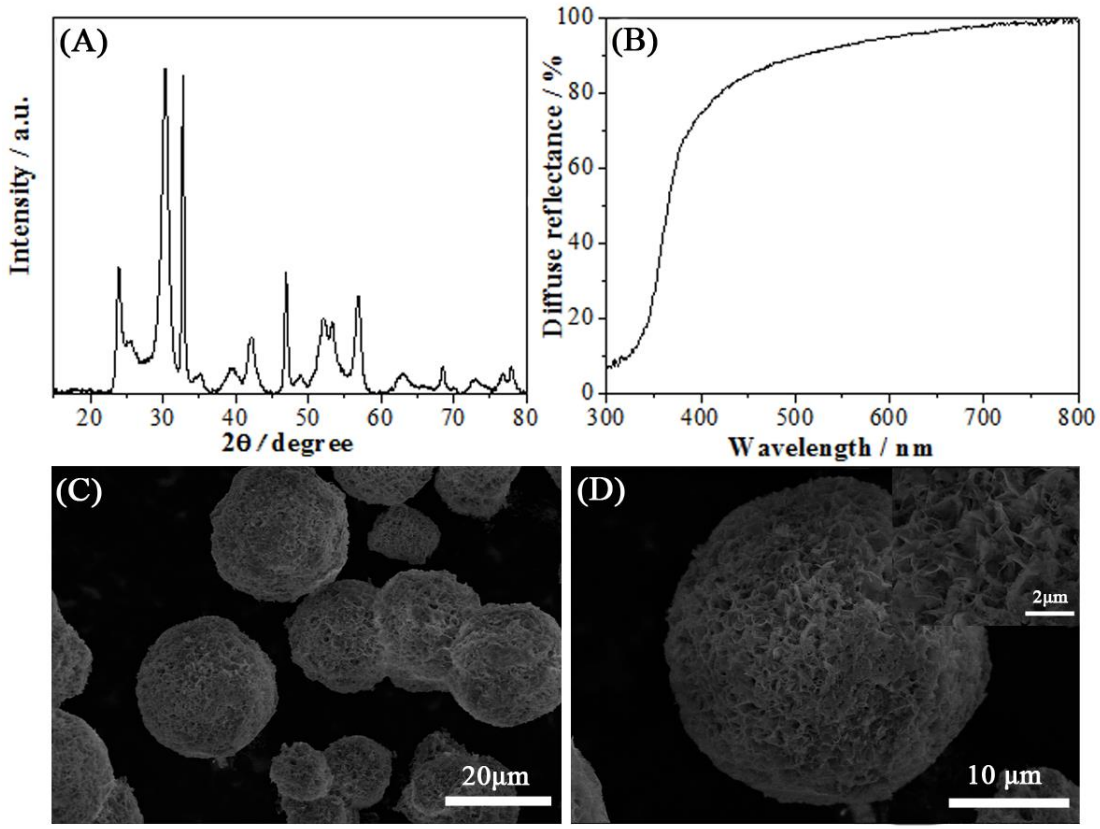

Figure S1 XRD patterns (A), UV-Vis DRS spectra (B), SEM images (C, D and inset of D) of $(BiO)_2CO_3$ precursor.

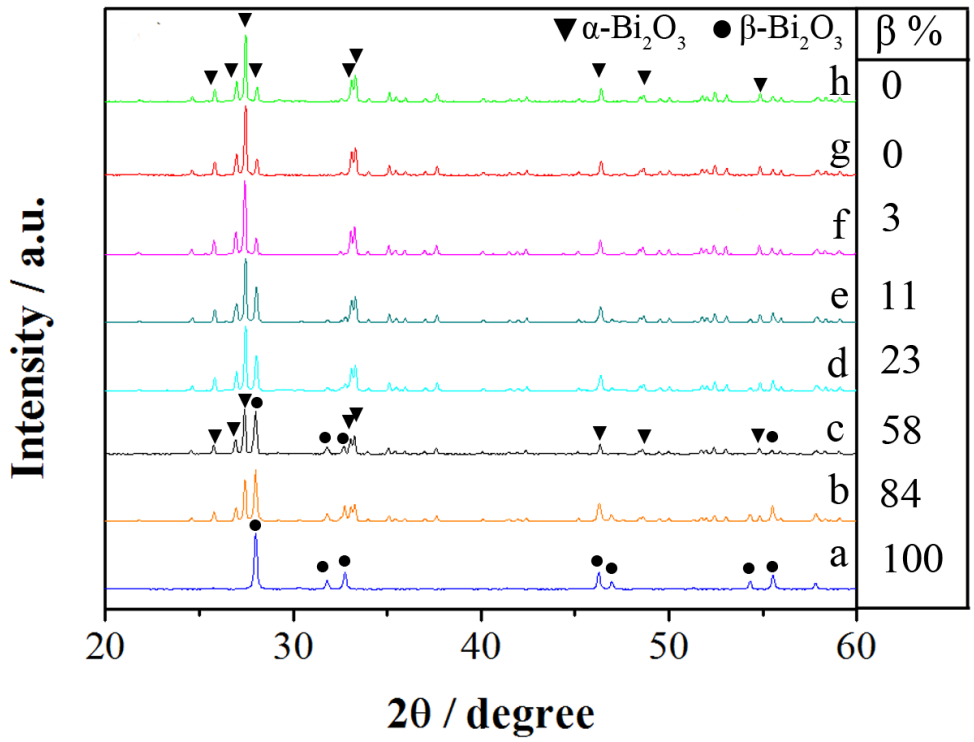

Figure S2 XRD patterns of sample a-h. (a-h stand for BO400, BO420, BO440, BO450, BO455, BO460, BO475 and BO500, respectively)

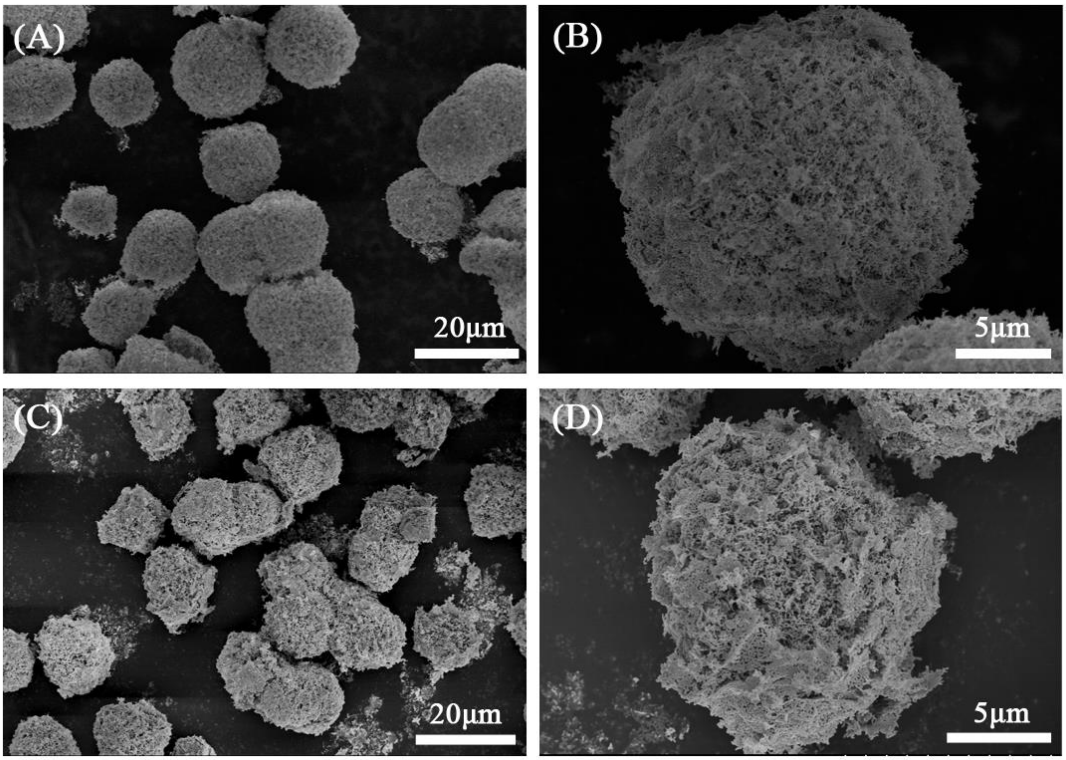

Figure S3 SEM images of BO400 (A, B) and BO500 (C, D).

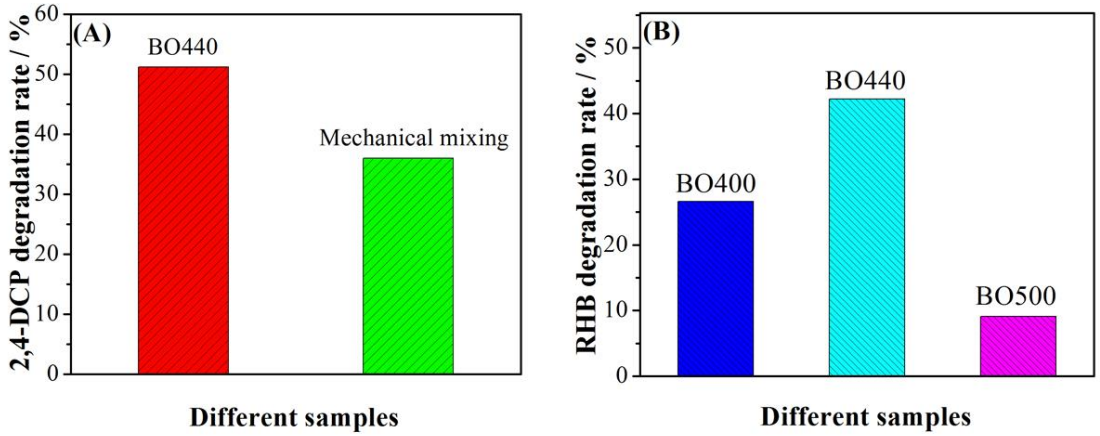

Figure S4 Photocatalytic degradation of 2,4-DCP of BO440 and mechanically mixed sample with the same mass ratios to BO440 under visible light irradiation (A) and Photocatalytic degradation of RhB of BO400, BO440 and BO500 under visible light irradiation; 0.02 g catalyst, 100 mL of 15 mg·L^{-1} RhB, 1 h irradiation (B).

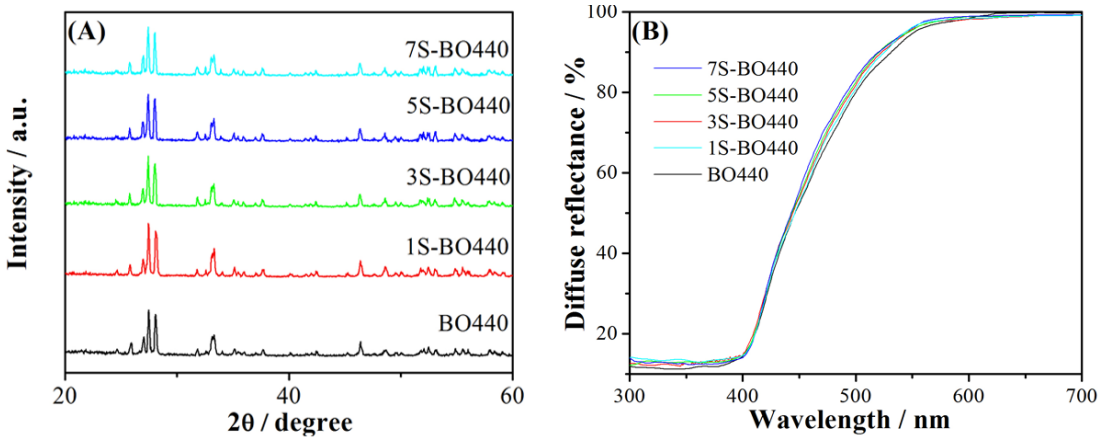

Figure S5 XRD patterns (A), DRS spectra (B) of BO440 and XS-BO440. (X represents different mass ratio of SnO_2 coupling on Bi_2O_3 and S refers to SnO_2)

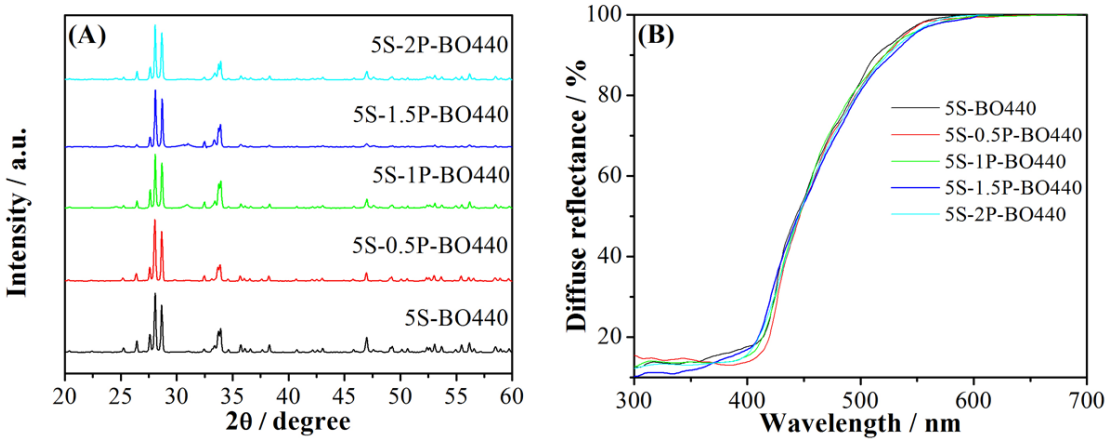

Figure S6 XRD patterns (A) and DRS spectra (B) of 5S-BO440 and 5S-YP-BO440. (Y represents the mass ratio of NaH_2PO_4 to Bi_2O_3)

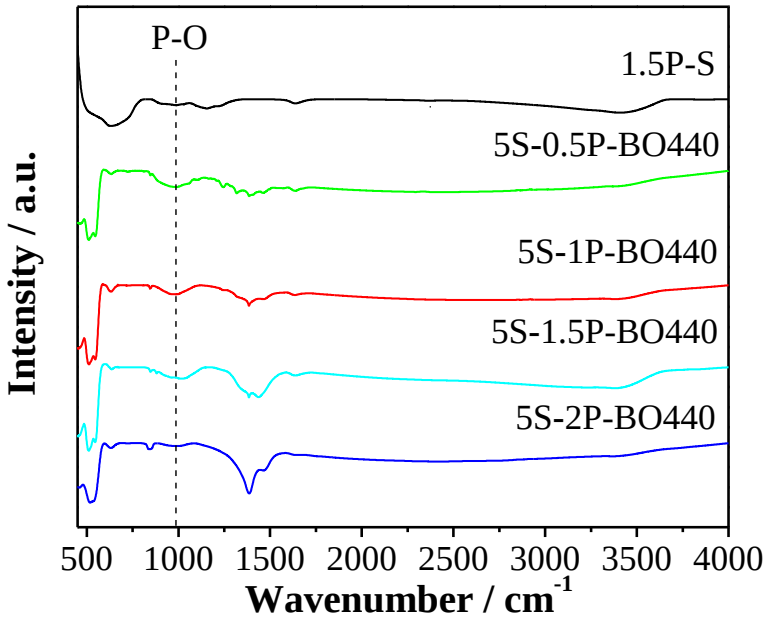

Figure S7 FT-IR spectra of 1.5P-S and 5S-YP-BO440.

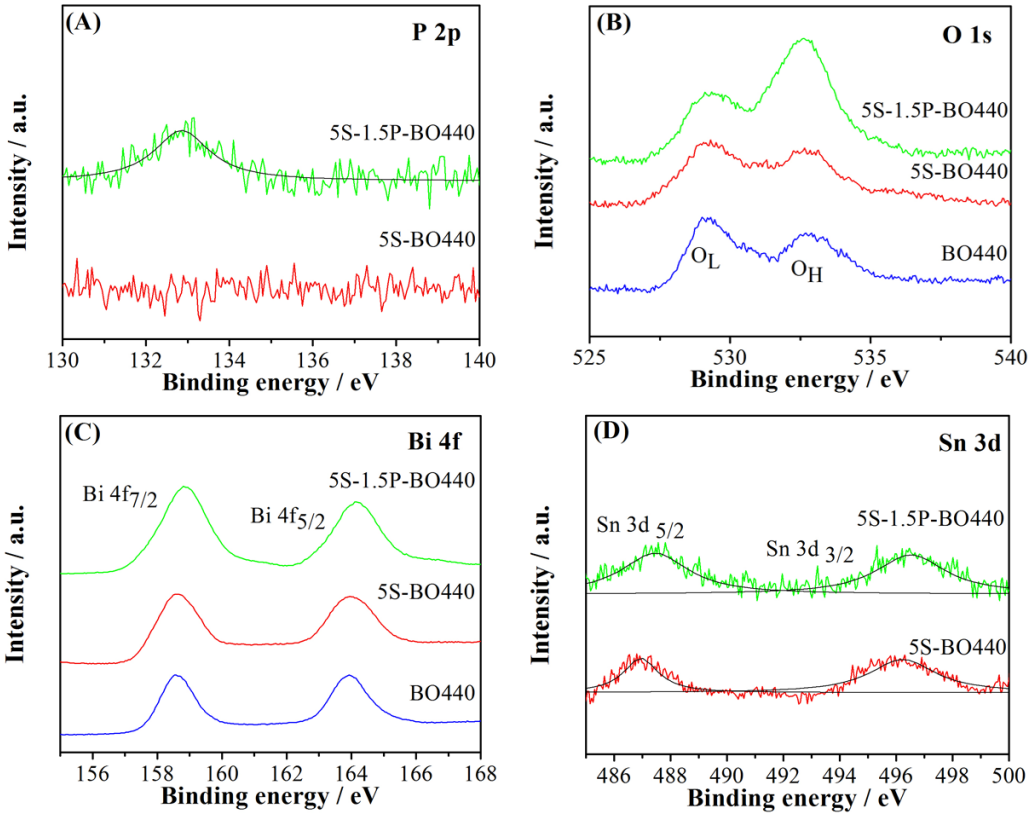

Figure S8 High resolution XPS spectra of BO440, 5S-BO440 and 5S-1.5P-BO440.

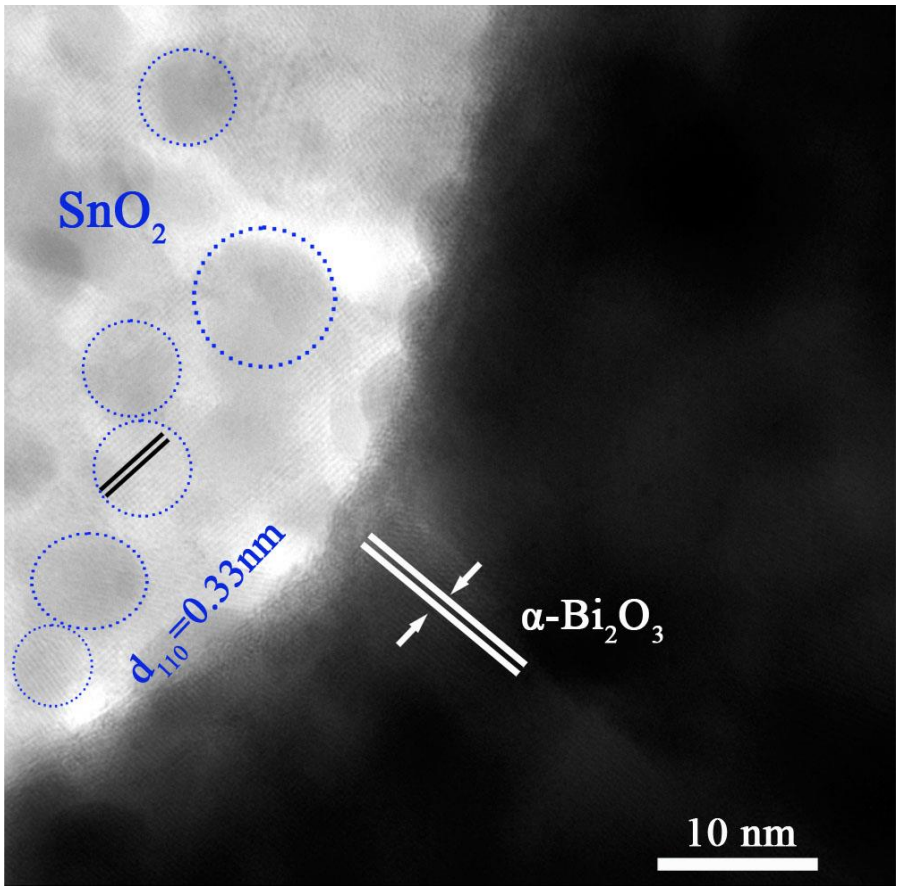

Figure S9 HRTEM image of 5S-BO440.

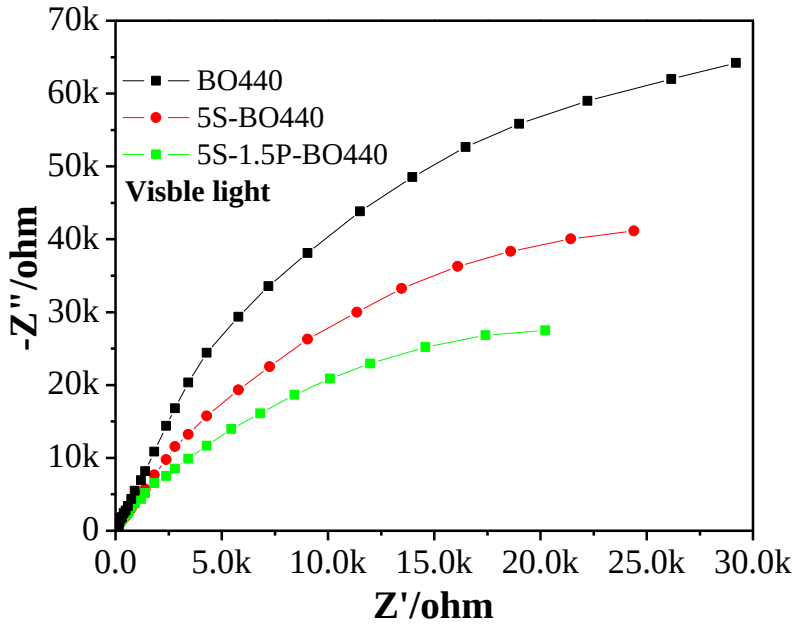

Figure S10 Electrochemical impedance spectra of BO440, 5S-BO440 and 5S-1.5P-BO440 samples.

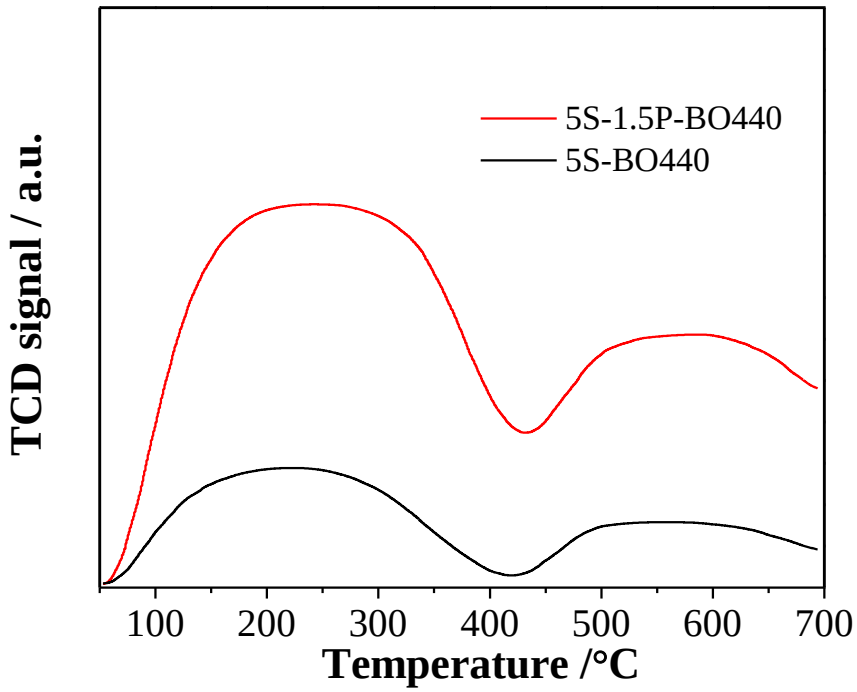

Figure S11 Corrected curves of O_2 temperature-programmed desorption on 5S-BO440 and 5S-1.5P-BO440.

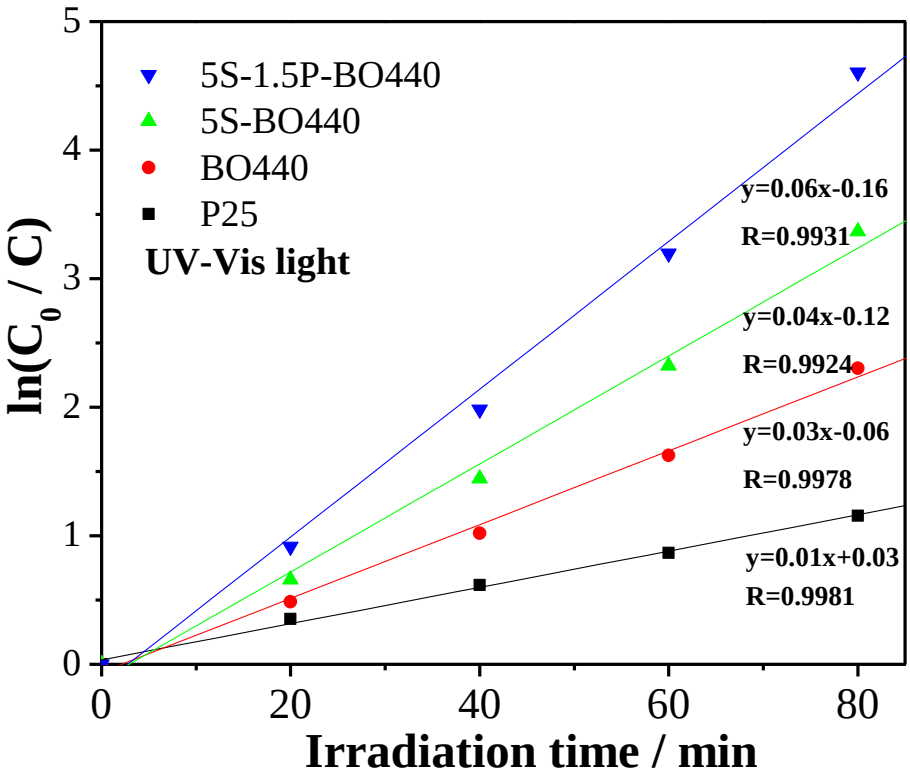

Figure S12 Pseudo-first-order decay curves of photocatalytic 2,4-DCP degradation over P25 TiO_2, BO440, 5S-BO440 and 5S-1.5P-BO440.

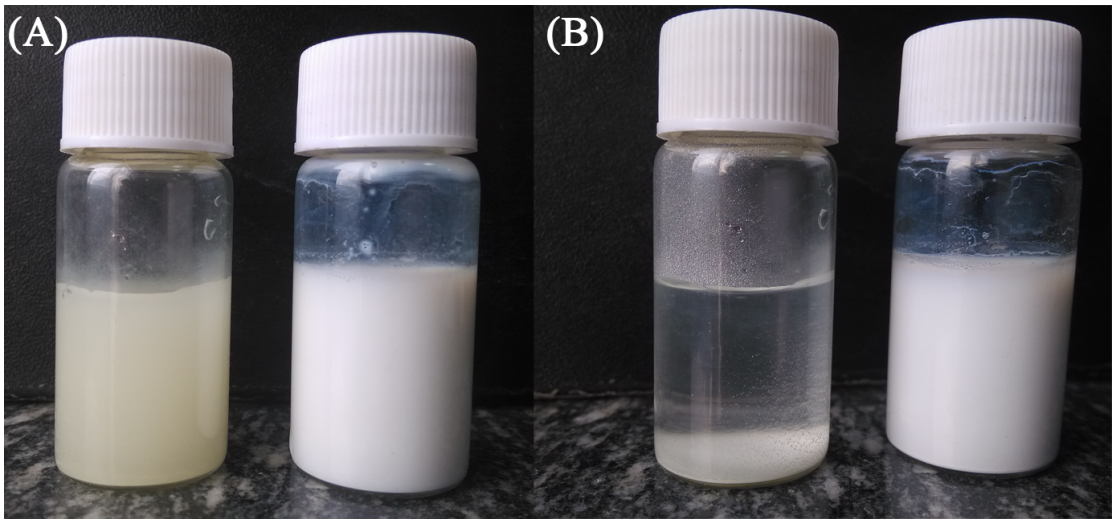

Figure S13 Self-separation effects of 5S-1.5P-BO440 (left) and P25 TiO_2 (right) in 2,4-DCP; just after stirring (A) and standing for 30 min (B).

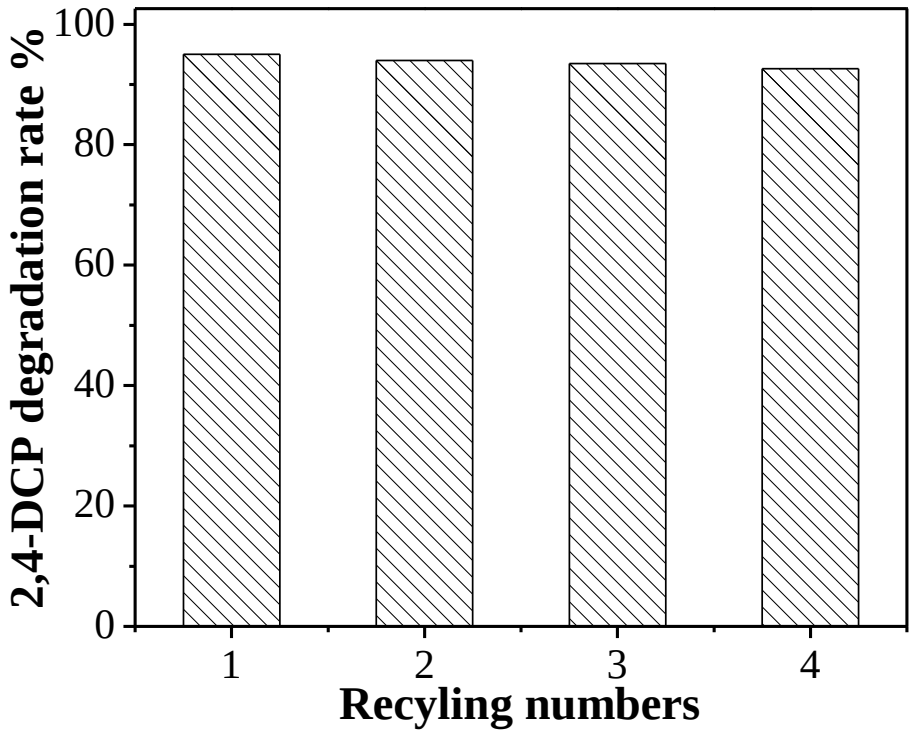

Figure S14 Recycle experiments of the self-separated 5S-1.5P-BO440.

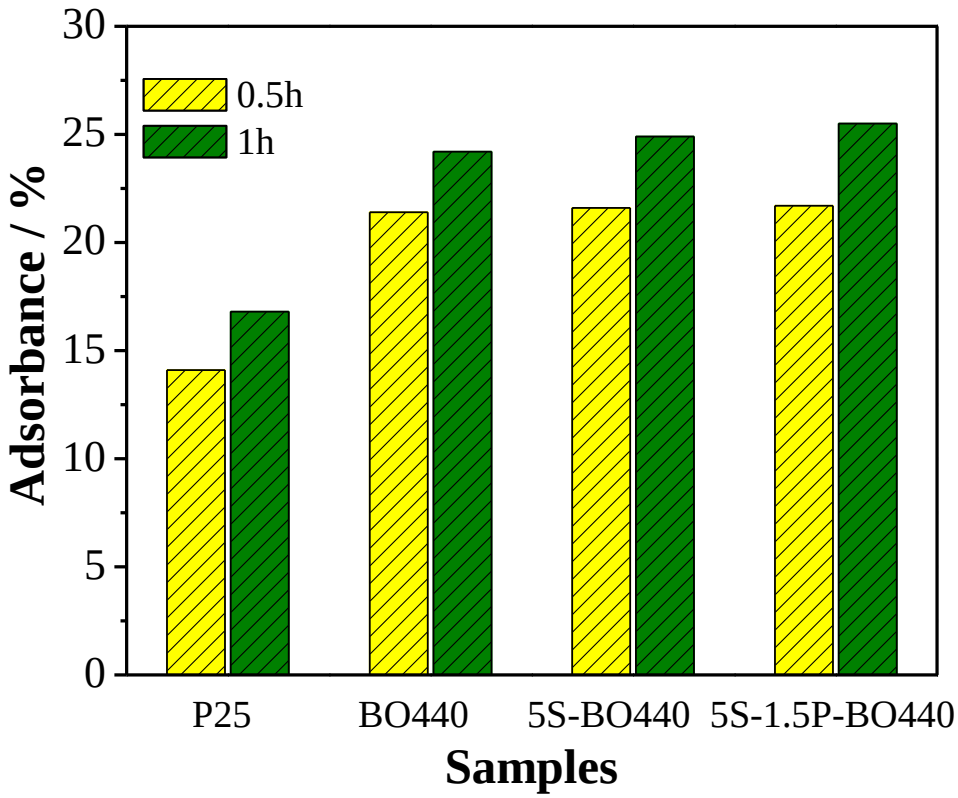

Figure S15 Adsorbance of 2,4-DCP for P25, BO440, 5S-BO440 and 5S-1.5P-BO440 at 0.5h and 1h in dark.

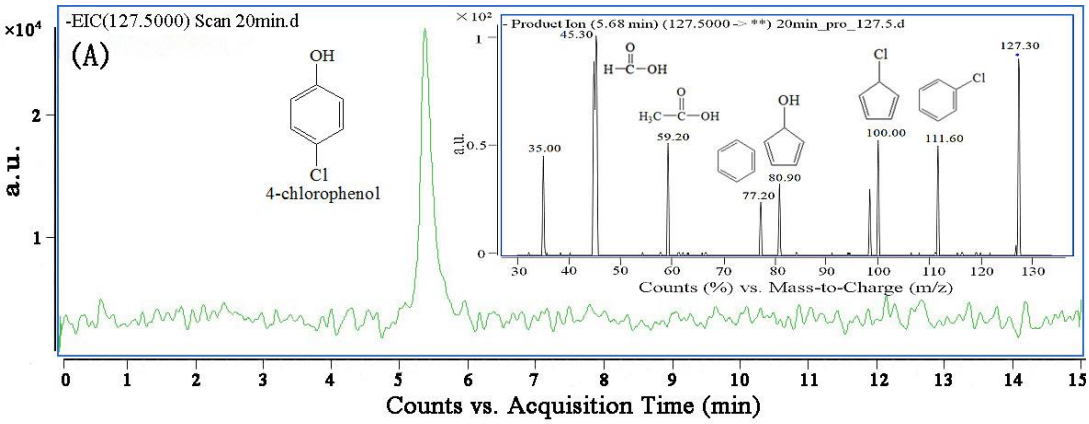
-EIC(127.5000) Scan 20min.d
(A)
4-chlorophenol
- Product Ion (5.68 min) (127.5000 -> **) 20min_pro_127.5.d
Counts (%) vs. Mass-to-Charge (m/z)
Counts vs. Acquisition Time (min)

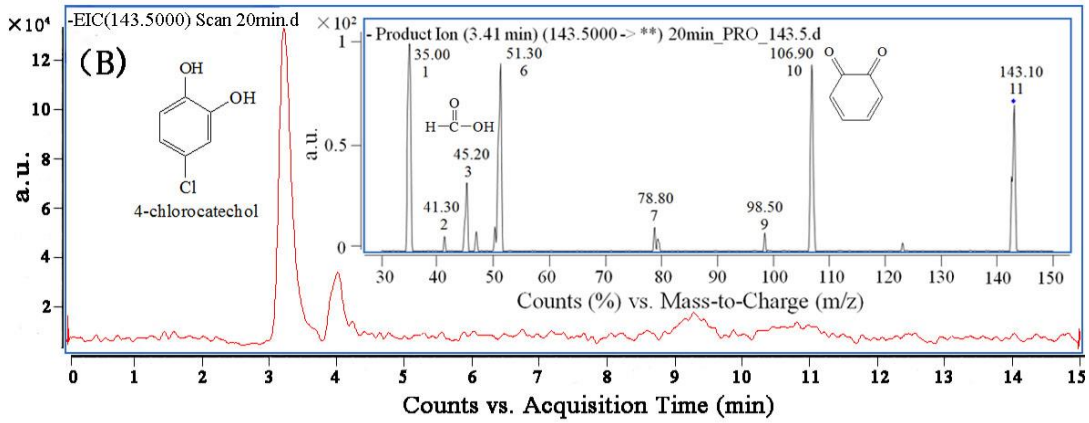
-EIC(143.5000) Scan 20min.d
(B)
4-chlorocatechol
- Product Ion (3.41 min) (143.5000 -> **) 20min_PRO_143.5.d
Counts (%) vs. Mass-to-Charge (m/z)
Counts vs. Acquisition Time (min)

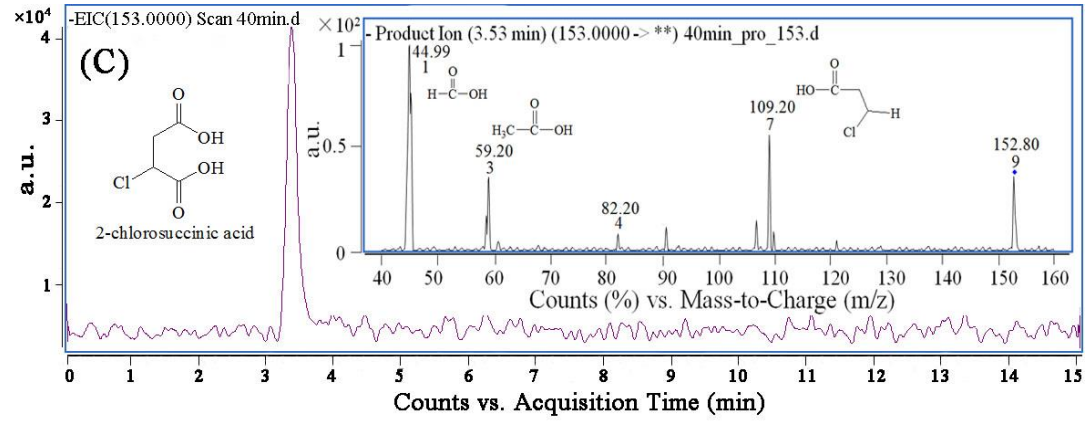
-EIC(153.0000) Scan 40min.d
(C)
2-chlorosuccinic acid
- Product Ion (3.53 min) (153.0000 -> **) 40min_pro_153.d
Counts (%) vs. Mass-to-Charge (m/z)
Counts vs. Acquisition Time (min)

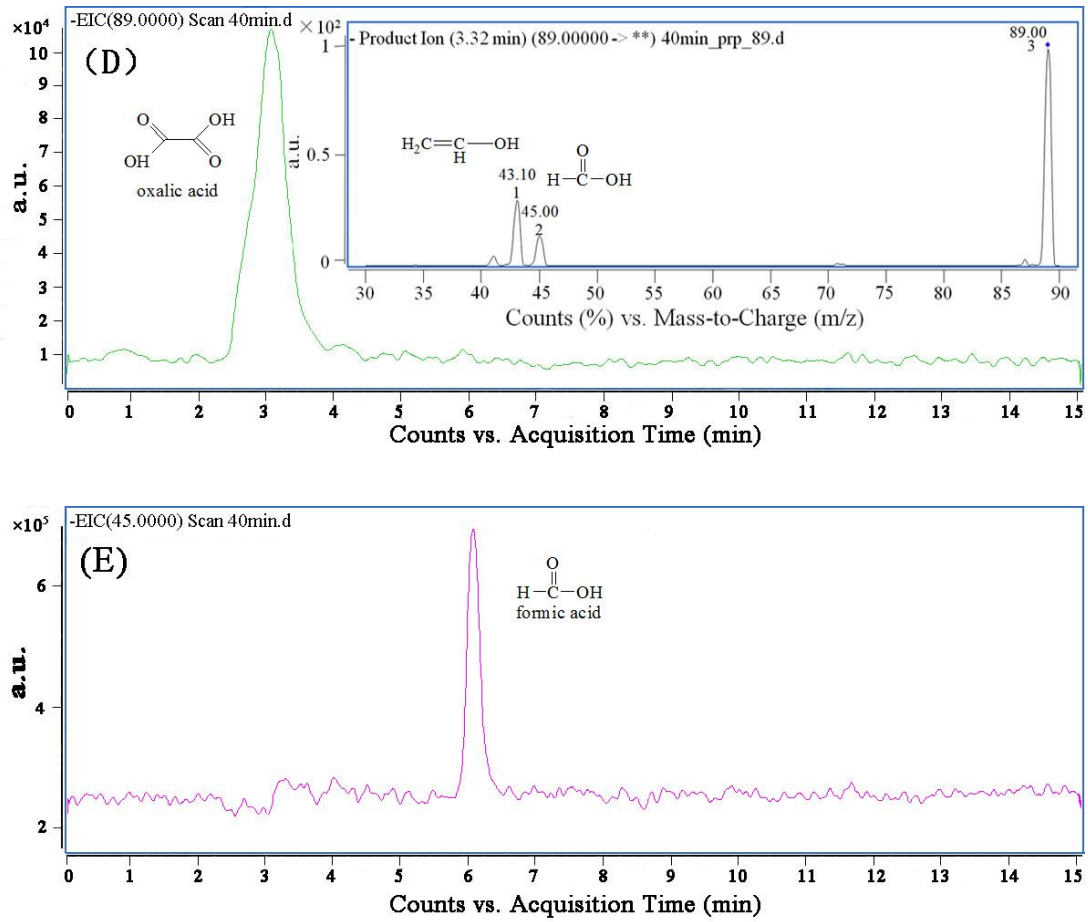

Figure S16 Extract ion chromatography (EIC) analysis of the intermediate products after UV-visible light catalytic degradation of 2,4-DCP over 5S-1.5P-BO440 photocatalyst at 20 and 40 min. The identified intermediate products, 4-chlorophenol (A), 4-chlorocatechol (B), 2-chlorosuccinic acid (C), oxalic acid (D) and formic acid (E).

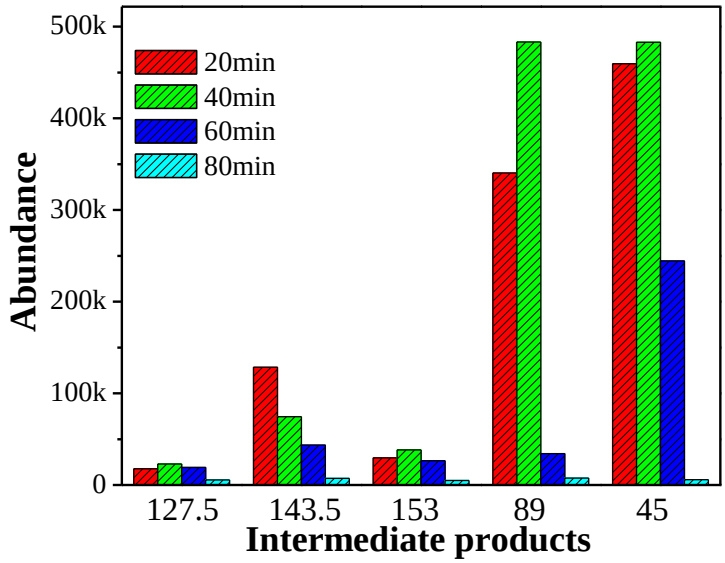

Figure S17 Liquid chromatography tandem mass spectrometry analyses of the resultant intermediate products during the UV-visible-light photocatalytic degradation of 2,4-DCP over 5S-1.5P-BO440 catalyst at different irradiation periods i.e. 20, 40, 60 and 80 min.

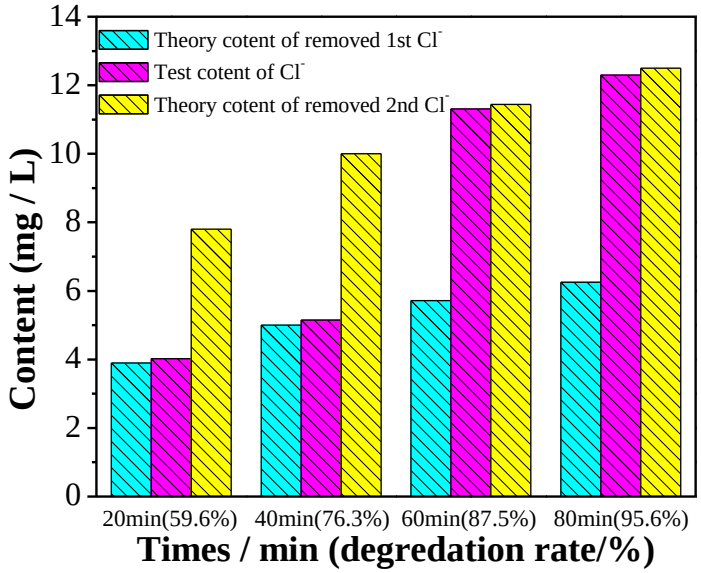

Figure S18 The chloride ion concentration of 5S-1.5P-BO440 at different reactive time of 20, 40, 60 and 80 min.

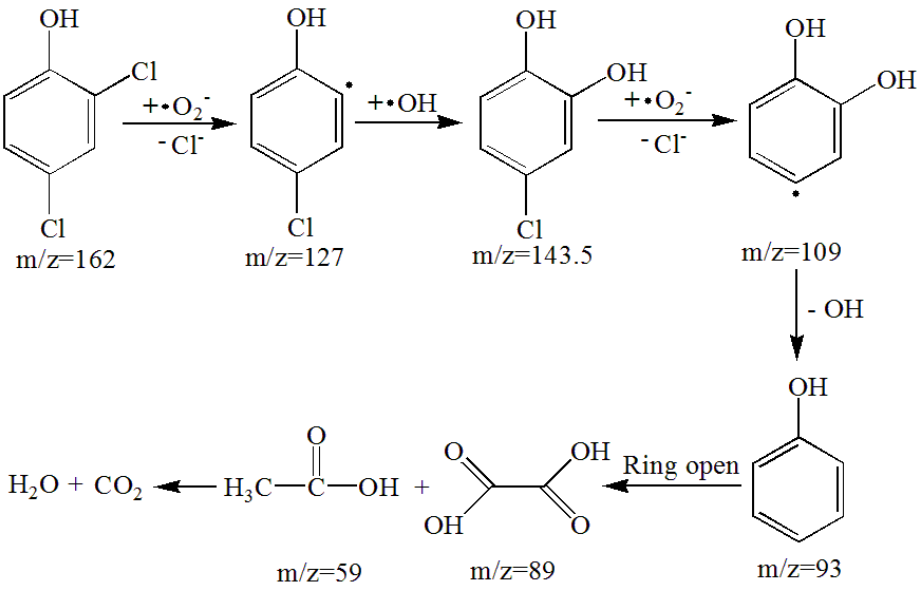

Scheme S1 Proposed pathway for 2,4-DCP degradation over P25 TiO_2 photocatalyst.

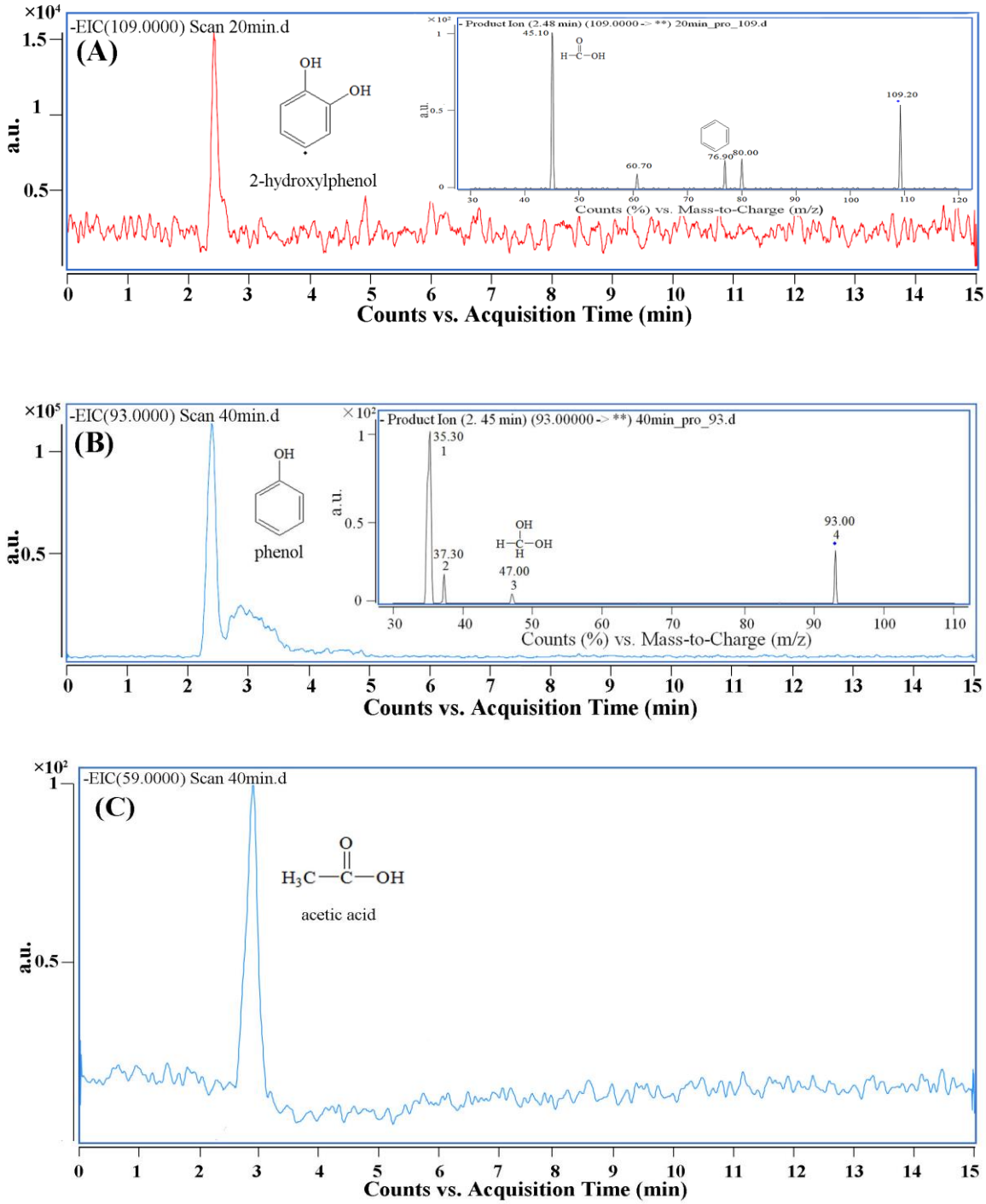

Figure S19 Extract ion chromatography (EIC) analysis of the intermediate products after UV-visible-light catalytic degradation of 2,4-DCP over P25 photocatalyst at 20 and 40 min. The identified intermediate products, 2-hydroxylphenol (A), phenol (B) and acetic acid (C).

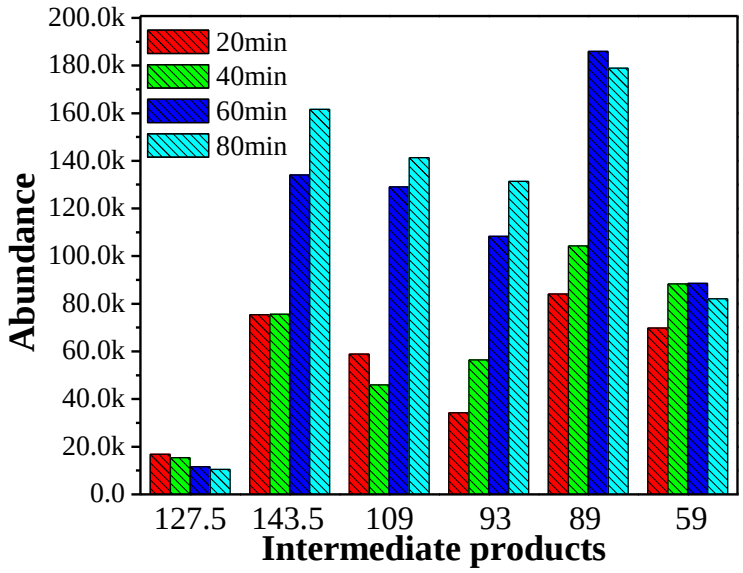

Figure S20 Liquid chromatography tandem mass spectrometry analyses of the resultant intermediate products during the UV-visible light photocatalytic degradation of 2,4-DCP over P25 catalyst at different irradiation periods i.e. 20, 40, 60 and 80 min.

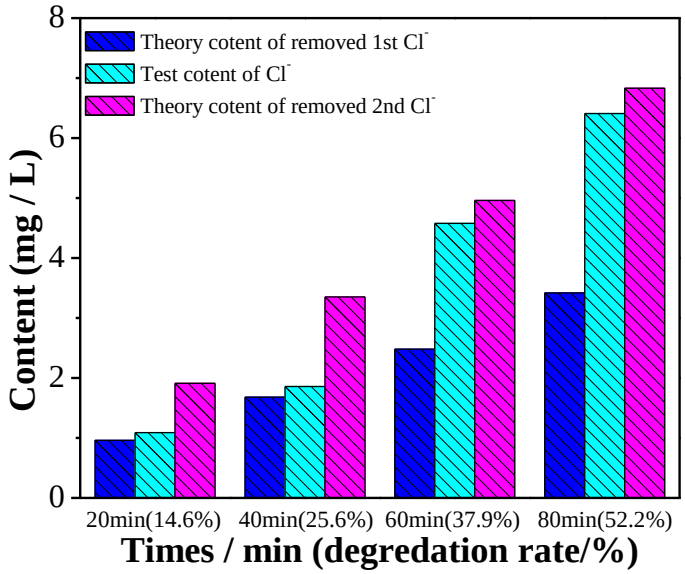

Figure S21 The chloride ion concentration of P25 at different reactive time of 20, 40, 60 and 80 min.